J|A|C|S
COMMUNICATIONS

Published on Web 05/12/2006

Mesoporous Silica−Magnetite Nanocomposite: Fabrication and Applications in Magnetic Bioseparations

Tapas Sen,* Antonio Sebastianelli, and Ian James Bruce

Department of Biosciences, University of Kent at Canterbury, Canterbury, Kent, CT2 7NJ, United Kingdom

Received March 8, 2006; E-mail: t.sen@kent.ac.uk

Fabrication of nanomaterials using "bottom-up"[1] approaches is key to developing structured, efficient materials on nanometer length scales, and nanotechnology is an emerging field beginning to impinge on many aspects of bio/life sciences,[2] such as tissue engineering, gene targeting, tumor therapy, diagnostics, etc. In this context, magnetic carrier technology (MCT), first reported by Robinson et al. in 1973,[3] has become an increasingly popular tool for bioseparations[4−7] and molecular diagnostics, especially immunoassays, for example, Dynabeds antilisteria (Dynal Biotech, Oslo, Norway). We have previously reported[8,9] various hierarchically ordered porous materials using template-assisted synthesis; however, the materials lacked magnetic properties for applications in magnetic bioseparations. Mesoporous silica−magnetite materials were first reported by Wu et al.,[10] but the materials were irregular in shape and size. Recently, Zhao et al.[11] have reported the fabrication of magnetic mesoporous core−shell nanomaterial of spherical morphology.

Herein we report the template-assisted fabrication of magnetic mesoporous silica−magnetite nanocomposite and its potential for application in magnetic bioseparations, that is, its ability (i) to bind and elute DNA and (ii) extract RNA from bacterial cells.

Magnetite nanoparticles were synthesized by the method of Sugimoto,[12] which were then used as a core material for the fabrication of mesoporous magnetic nanocomposite. In a typical synthesis, a gel containing a surfactant (cetyl trimethylammonium bromide, CTAB), a source of silica (tetra ethyl orthosilicate, TEOS), and sodium hydroxide (NaOH) was added to a magnetite suspension in water while stirring at room temperature. The pH of the mixture was adjusted to 7 by slow addition of 2 M HCl solution over a period of 30 min, and the resultant particles were washed several times in water followed by ethanol to remove the surfactant molecules.

When analyzed, the core material exhibited an XRD pattern (Figure 1a) corresponding to pure magnetite[13] without any impurity of maghemite or hematite. The nanocomposite exhibited an additional low angle peak ($* = d$ value 3.8 nm) along with multiple peaks in the high angle region (Figure 1b). The low angle peak present in nanocomposite suggests mesoporous silica[14] without much indication of ordering, while the multiple high angle peaks relate to the magnetite core.

SEM micrographs (Figure 2) of core and silica−magnetite composite showed that they were aggregated nanocrystals lacking precise structure. TEM micrographs of the core material indicated rhombic crystals with sizes ranging from 30 to 150 nm, and the nanocomposite was observed to exhibit both spherical and rod-shaped morphologies. In all cases, the core was composed of the rhombic magnetite nanocrystals, while the shell was formed by mesoporous silica. The thickness of the mesoporous silica shell on the nanospheres was observed to be in the range of 10−20 nm with a pore diameter of around 3.5 nm. This result corresponds well to the *d* value obtained from XRD. The diameter of the

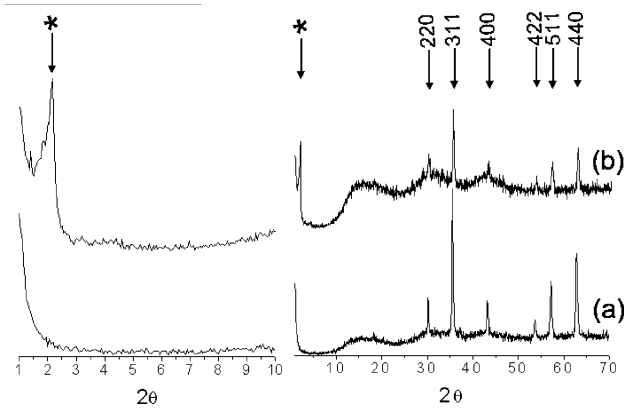

Figure 1. XRD pattern of core (a) and silica−magnetite nanocomposites (b) of low angle region (left traces) and full region (right traces).

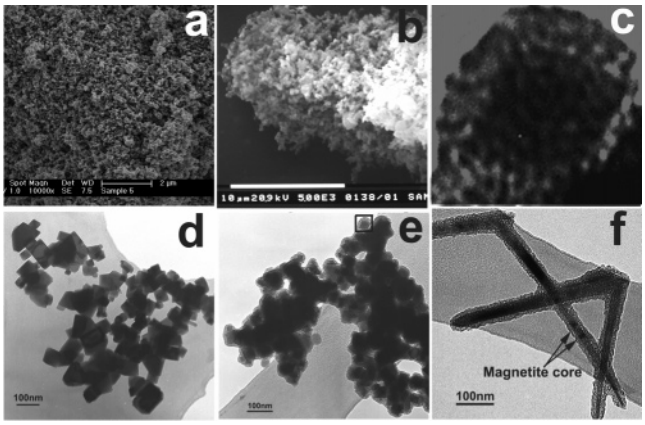

Figure 2. Electron micrographs of various samples: core magnetite (a, SEM; d, TEM), mesoporous silica−magnetite nanocomposite (b, SEM; e, TEM; c, selected region of e; and f, nanorod).

nanorods was observed to be around 50 nm. The size of the *encapped* magnetite nanocrystals within the nanorods was <35 nm. The relative amount of rod-shaped to spherical morphology was observed to be less than 10%. The pore size of the mesoporous silica shell could be controlled by varying the micelle sizes by using different surfactants.

FT-IR analysis of the core and the nanocomposite indicated an absorption centered at 580 cm^{-1} corresponding to the Fe−O^- vibration[15] related to the magnetite phase (see Supporting Information, Figure S1). The presence of additional peaks centered at 800, 968, 1075, and 1225 cm^{-1} were most probably due to the symmetric and asymmetric stretching vibration of framework and terminal Si−O^- groups.[16]

The temperature dependence of the static magnetic susceptibility of core magnetite and the nanocomposite was measured, and the saturation magnetization (Ms) for both was observed to center at 88 emu/g at 2.5 K and around 82 emu/g at 300 K. These results

10.1021/ja061393q CCC: $33.50

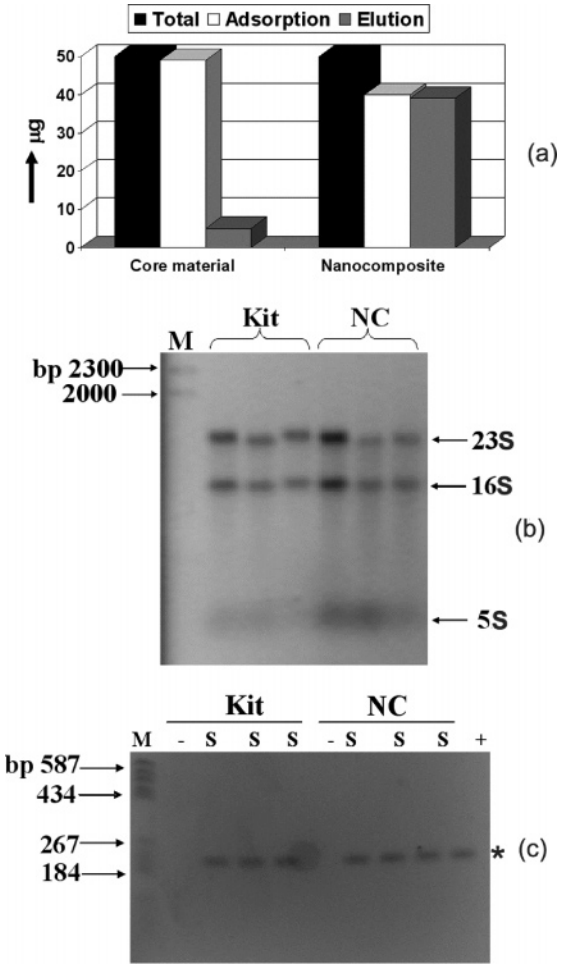

Figure 3. Binding and elution of salmon sperm DNA (a), totRNA extraction from (b), reverse transcription PCR (c). M, sequence ladder; S, sample; −, negative control; +, positive control; NC, nanocomposite. ∗ indicates a *tfdA* gene fragment.

confirm that the magnetic properties of the core remained unchanged upon formation of nanocomposite.

BET surface area measurement of the magnetite core gave a value of 25m^2/g, and a large increase in this value to 250m^2/g was observed for the silica−magnetite nanocomposite. The observation of hysteresis and an increase of surface area are due to the mesoporous shell structure of the nanocomposite.

Binding and elution of sheared salmon sperm DNA to, and from, the mesoporous silica−magnetite nanocomposite, and core magnetite at physiological pH (7.2) under chaotropic conditions, that is, at high salt concentration, was studied, and the results are presented in Figure 3a. Both core magnetite and silica−magnetite nanocomposite demonstrated a high capacity for binding the DNA, whereas the recovery efficiency of adsorbed DNA was observed to be different. Nearly 100% recovery of DNA was obtained from the surface of the nanocomposite, whereas <10% was recovered from the magnetite core. It was possible to bind and elute approximately the same quantity of DNA using half the amount of the mesoporous silica−magnetite composite compared to classical amorphous silica−magnetite materials.[17] The binding mechanism of DNA on the surface of the nanocomposite is most likely to be electrostatic interactions between the negatively charged phosphate backbone of DNA with positively charged surface of nanoparticles at physiological pH in the presence of high salt concentration.[18]

The performance of the nanocomposite in extraction of RNA from bacterial cell (1×10^7 *B. cepacia* strain 2a) was assessed by comparing the total RNA (totRNA) extracted from cells against that using an "RNeasy Mini Kit" (Quiagen Ltd., Crawley, UK) which had been analyzed via reverse transcription (RT) PCR. Figure 3b shows that the quality and the quantity of totRNA (i.e., assessed via the presence of the ribosomal RNA-23S, 16S, and 5S bands)[19] extracted using nanocomposite was comparable with that obtained using a commercial kit. Moreover, a 230 bp fragment of the *tfdA* gene from *B. cepacia* strain 2a was amplifiable in both samples (Figure 3c) and confirmed that RNA extraction using the mesoporous nanocomposite did not impair the RNA quality or interfere with the amplification procedure. This was also demonstrated in the case of DNA sequencing in which the sequence of eluted plasmid DNA (*tfdA*) from nanocomposite was identical to that of pure plasmid DNA (*tfdA*) (see Supporting Information, Figure S2).

In conclusion, template-assisted mesoporous magnetic nanocomposite has been fabricated and efficiently applied in magnetic bioseparations.

Acknowledgment. The authors thank the European Commission for financial support under FP6 (NACBO 500804), and Dr. Enrico Borioni for DNA analysis.

Supporting Information Available: Details of experimental protocols for nanocomposite fabrication, salmon sperm DNA experiment, RNA extraction from bacterial cell, FT-IR data, plasmid DNA sequence data, and high-resolution electron micrographs of Figure 2. This material is available free of charge via the Internet at http://pubs.acs.org.

References

(1) Shimomura, M.; Sawadaishi, T. *Curr. Opin. Colloid Interface Sci.* **2001**, *6*, 11−16.
(2) Salata, O. V. *J. Nanobiotechnology* **2004**, *2*, 1−6.
(3) Robinson, P. J.; Dunnill, P.; Lilly, M. D. *Biotechnol. Bioeng.* **1973**, *15*, 603−606.
(4) Whitehead, R. A.; Chagnon, S.; Groman, E. V.; Josephson, L. U.S. Patent 4554088 (Advanced Magnetics Inc., U.S.), 1985.
(5) Safarik, I.; Safarikova, M. *J. Chromatogr. B* **1999**, *722*, 33−53.
(6) Sinclair, B. *Scientist* **1998**, *12*, 16.
(7) Nunez, L.; Kaminski, M. D. *Chemtech*. **1998**, *9*, 41−46.
(8) Sen, T.; Casci, J. L.; Tiddy, G. J. T.; Anderson, M. W. *Angew. Chem., Int. Ed.* **2003**, *42*, 4649−4653.
(9) Sen, T.; Casci, J. L.; Tiddy, G. J. T.; Anderson, M. W. *Chem. Mater*. **2004**, *16*, 2044−2054.
(10) Wu, P.; Zhu, J.; Xu, Z. *Adv. Funct. Mater*. **2004**, *14*, 345−351.
(11) Zhao, W.; Gu, J.; Zhang, L.; Chen, H.; Shi, J. *J. Am. Chem. Soc.* **2005**, *127*, 8916−8917.
(12) Sugimoto, T.; Matijevic, E. *J. Colloid Interface Sci*. **1980**, *74*, 227−243.
(13) Itoh, H.; Sugimoto, T. *J. Colloid Interface Sci*. **2003**, *265*, 283−295.
(14) Beck, J. S.; Vartuli, J. C.; Roth, W. J.; Leonowicz, M. E.; Kresge, C. T.; Schmitt, K. D.; Chu, C. T. W.; Olson, D. H.; Sheppard, E. W.; Mccullen, S. B.; Higgins, J. B.; Schlenker, J. L. *J. Am. Chem. Soc.* **1992**, *114*, 10834−10843.
(15) Sun, Z.; Su, F.; Forsling, W.; Samskog, P. *J. Colloid Interface Sci*. **1998**, *197*, 151−159.
(16) Chen, X.; Huang, L.; Li, Q. *J. Phys. Chem. B* **1997**, *101*, 8460−8467.
(17) Bruce, I. J.; Taylor, J.; Todd, J. M.; Davies, M. J.; Borioni, E.; Sangregorio, C.; Sen, T. *J. Magn. Magn. Mater*. **2004**, *284*, 145−160.
(18) Melzak, K. A.; Sherwood, C. S.; Turner, R. F. B.; Haynes, C. A. *J. Colloid Interface Sci.* **1996**, *181*, 635−644.
(19) Neidhardt, C. F.; Ingraham, J. C.; Schaechter, M. *Physiology of the Bacterial Cell: A Molecular Approach*; Sinauer Associates Inc.: Sunderland, MA, 1990.

JA061393Q